RSC Advances

PAPER

View Article Online
View Journal | View Issue

Cite this: *RSC Adv.*, 2020, **10**, 18434

A simple fluorescent probe for detection of Ag^+ and Cd^{2+} and its Cd^{2+} complex for sequential recognition of S^{2-}†

Shengling Li,[a] Duanlin Cao,[a] Wenbing Ma,*[ab] Zhiyong Hu,[ab] Xianjiao Meng,[c] Zhichun Li,[a] Changchun Yuan,[a] Tao Zhou[a] and Xinghua Han[ab]

Received 24th February 2020
Accepted 7th May 2020

DOI: 10.1039/d0ra01768j

rsc.li/rsc-advances

In this study, we designed and synthesized a simple probe 2-(8-((8-methoxyquinolin-2-yl)methoxy) quinolin-2-yl)benzo[*d*]thiazole (**DQT**) for detection of Ag^+ and Cd^{2+} in a CH_3OH/HEPES (9 : 1 v/v, pH = 7.30) buffer system. Its structure was characterized by NMR, ESI-HR-MS and DFT calculations, and its fluorescence performance was also investigated. Probe **DQT** showed fluorescence quenching in response to Ag^+ and Cd^{2+} with low detection limits of 0.42 μM and 0.26 μM, respectively. Importantly, the complexation of the probe with Cd^{2+} resulted in a red shift from blue to green, making it possible to detect Ag^+ and Cd^{2+} by the naked eye under an ultraviolet lamp. The **DQT**-Cd^{2+} complex could be used for sequential recognition of S^{2-}. The recovery response could be repeated 3 times by alternate addition of Cd^{2+} and S^{2-}. A filter paper strip test further demonstrated the potential of probe **DQT** as a convenient and rapid assay.

Introduction

Cd^{2+} and Ag^+ ions are important transition metal ions involved in various biological and environmental processes.[1–4] However, excessive intake of Ag^+ can cause serious harm to human health as it can inactivate thiolase and even have a carcinogenic effect.[5,6] Cd^{2+} is one of the most serious air pollutants, and it is also highly toxic, causing serious health problems even at low concentrations.[7–10] It is reported that Cd^{2+} ions are associated with the pathogenesis of many diseases including cancers.[11–14] Thus, it is necessary to detect Cd^{2+} and Ag^+ in the environment. However, traditional methods such as capacity analysis,[15] ICP-MS[16] and atomic absorption method,[17] may be greatly limited due to requirement of equipment, high cost, cumbersome operation and low accuracy.[18] In comparison, the fluorescence detection method has advantages of high specific recognition ability, high sensitivity and short response time, making it useful for the detection of many metal ions such as Hg^{2+}, Pb^{2+}, Cu^{2+} and Zn^{2+}.[19–23]

Two mechanisms namely PET and ICT are inclusively used as the basis for the design of fluorescent probes.[24–26] PET refers to the process of fluorescence quenching or enhancement caused by electron transfer between the excited electron donor or electron acceptor after photoexcitation.[27] In addition, the recognition groups of ICT probes are usually a part of the push–pull electron system, and thus the combination of these groups with metal ions may affect the push–pull electron effect of the fluorophore and the intramolecular charge transfer, thus leading to changes in fluorescence spectrum.[28]

Many fluorescent probes have been developed based on the two mechanisms for the detection of a variety of ions, such as Cu^{2+}/Cd^{2+},[29,30] Zn^{2+}/Cd^{2+},[31–33] and Cu^{2+}/Cd^{2+}/PPi.[34] However, there are fewer probes for the detection of Ag^+/Cd^{2+}/S^{2-}. In this work, a simple fluorescent probe **DQT** was successfully synthesized based on quinolone[35–38] and benzothiazole,[39–41] which showed high selectivity toward Ag^+ and Cd^{2+} in CH_3OH/HEPES (9 : 1 v/v, pH = 7.30), and its Cd^{2+} complex could be

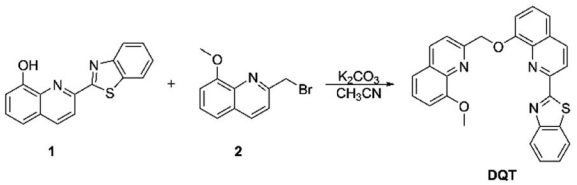

Scheme 1 Synthesis of probe **DQT**.

[a]*School of Chemical Engineering and Technology, North University of China, Taiyuan 030051, P.R. China. E-mail: mawenbing@nuc.edu.cn*

[b]*National Demonstration Center for Experimental Comprehenisve Chemical Engineering Education, North University of China, Taiyuan 030051, P.R. China*

[c]*College of Arts and Sciences, Shanxi Agricultural University, Taigu, Shanxi, 030801, P.R. China*

† Electronic supplementary information (ESI) available: Appendix A includes the Experimental section, ^{1}H NMR spectra, ^{13}C NMR spectra, ESI-MS spectra and part of spectrums of probe **DQT**; Appendix B includes the detail crystal data, structure refinement, torsion angles and bond lengths and angles of probe **DQT**. CCDC 1975779. For ESI and crystallographic data in CIF or other electronic format see DOI: 10.1039/d0ra01768j

used for sequential recognition of S^{2-}. The paper strip test was carried out to verify its practicability (Scheme 1).

Results and discussion

X-ray structural analysis probe DQT

As shown in Fig. 1, the crystal structure without hydrogen atom of probe **DQT** was given. The cell parameters were $a = 21.767(3)$ Å, $\alpha = 90$ deg; $b = 4.8042(8)$ Å, $\beta = 103.866(7)$ deg; $c = 42.042(7)$ Å, $\gamma = 90$ deg. The detail crystal data, structure refinement, torsion angles and bond lengths and angles for probe **DQT** were shown in Tables S1–S3 of Appendix B.† More information has been uploaded to the Cambridge Crystallographic Date Center (CCDC 1975779).

The fluorescence response of probe DQT towards Ag^+ and Cd^{2+}

To study the fluorescence selectivity of probe **DQT** toward metal ions, the fluorescence spectra of probe **DQT** upon the addition of 20 equiv. of K^+, Na^+, Zn^{2+}, Cu^{2+}, Hg^{2+}, Pb^{2+}, Ba^{2+}, Cd^{2+}, Cs^+, Li^+, Ag^+, Mg^{2+}, Ca^{2+}, Al^{3+}, Ni^{2+} and Fe^{3+} were recorded in CH_3OH/HEPES (9 : 1 v/v, pH = 7.30) ($\lambda_{ex} = 344$ nm). As shown in Fig. 2(a), no distinct changes were observed in fluorescence spectra of probe **DQT** ($\Phi = 0.308$) upon the containing of metal cations except that with the presence of Ag^+ ($\Phi = 0.002$) and Cd^{2+} ($\Phi = 0.227$). Upon the addition of different metal ions, Ag^+ caused a 88% fluorescence quenching and displayed an "on–off" behavior. With Cd^{2+}, probe **DQT** showed a 33% fluorescence quenching with a spectral red-shift of 25 nm from 465 to 490 nm. This could be attributed to changes in the electronically conjugated structure of the molecule after the combination of the lone pair of electrons of N atoms with Cd^{2+}. In addition, due to the special molecular configuration and electronic structure of the compound, complex **DQT**-Cd^{2+} was not interfered by other ions. Apparent color changes were observed, indicating that probe **DQT** could be used to detect Ag^+ and Cd^{2+} by naked eye (Fig. 2(b) and (c)).

Competition experiments were performed to explore the effects of other metal ions on the recognition of Ag^+ and Cd^{2+}. It could be seen in Fig. 3(a) that there was significant change in fluorescence intensity after the addition of 20 equiv. of Ag^+. Clearly, the recognition of Ag^+ was affected by these metal ions. However, the recognition of Cd^{2+} was not affected especially Ag^+ and the fluorescence color was still green under UV light, as

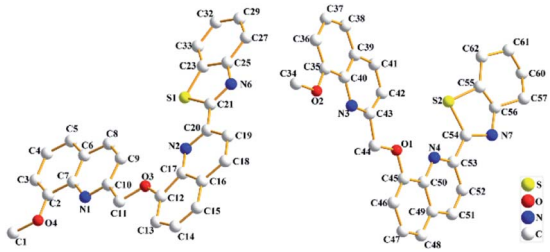

Fig. 1 The crystal structure without hydrogen atom of probe **DQT**.

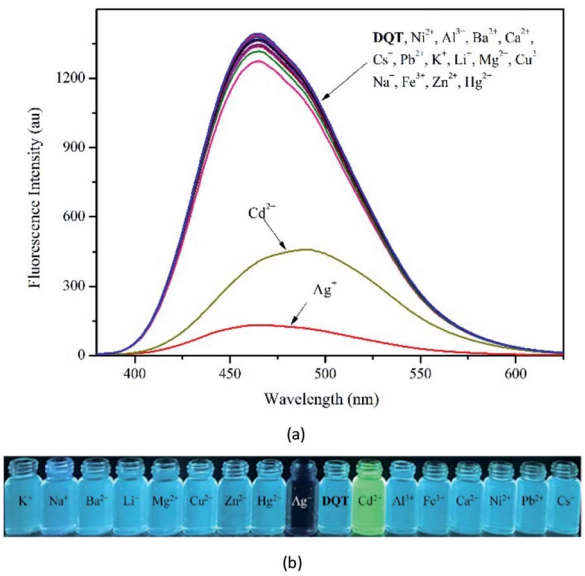

Fig. 2 (a) Fluorescence spectra of probe **DQT** upon the addition of various metal cations (2×10^{-4} mol L^{-1}) and blank. (b) Color changes of probe **DQT** with various metal cations in CH_3OH/HEPES (9 : 1 v/v, pH = 7.30) buffer system under UV light.

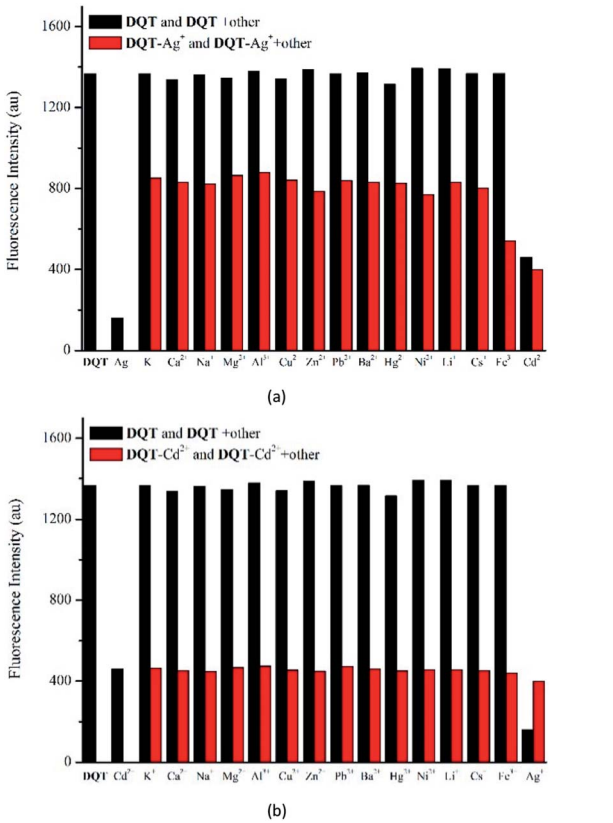

Fig. 3 Competitive selectivity of probe **DQT** (10 μM) toward Ag^+ (a) and Cd^{2+} (b) (20 equiv.) in the absence (black bars) or presence (red bars) of specified ions (20 equiv.).

shown in Fig. 3(b). Compared to Ag^+, probe **DQT** had higher selectivity for Cd^{2+}.

To better understand the sensitivity of probe **DQT** toward Ag^+ and Cd^{2+}, the fluorescent titration of Ag^+ and Cd^{2+} was carried out in CH_3OH/HEPES (9 : 1 v/v, pH = 7.30) buffer system at an excitation wavelength of 344 nm. As shown in Fig. 4(a), probe **DQT** exhibited an emission at 465 nm with an enormous Stokes shift of 121 nm. Upon incremental addition of Ag^+, the fluorescence emission gradually decreased until a plateau was reached at 20 equiv. of Ag^+. The limit of detection (LOD) was determined to be 0.42 μM based on LOD = $3\sigma/m$ (Fig. S6†). As shown in Fig. 4(b), the addition of Cd^{2+} resulted in a red shift of the fluorescence emission of probe **DQT** to 490 nm, and probe **DQT** showed fluorescence quenching with a LOD of 0.26 μM for Cd^{2+} (Fig. S7†). The stoichiometry determined by the Job's method was 1 : 1 for both **DQT**-Ag^+ and **DQT**-Cd^{2+} complexes, as shown at the upper right corner of Fig. 4(a) and (b). The complexation constant of probe **DQT** to Ag^+ ($K_a = 2.68 \times 10^3$ M^{-1}) (Fig. S4,† $Y = 1.75 \times 10^{-7} \times X - 4.69 \times 10^{-4}$, $R^2 = 0.9953$) obtained according to the Benesi–Hildebrand plots was lower than that to Cd^{2+} ($K_a = 2.23 \times 10^4$ M^{-1}) (Fig. S6,† $Y = 3.91 \times 10^{-8} \times X + 8.72 \times 10^{-4}$, $R^2 = 0.9967$). The titration results were consistent with the interference results, indicating that probe **DQT** had a better sensitivity for Cd^{2+} than Ag^+.

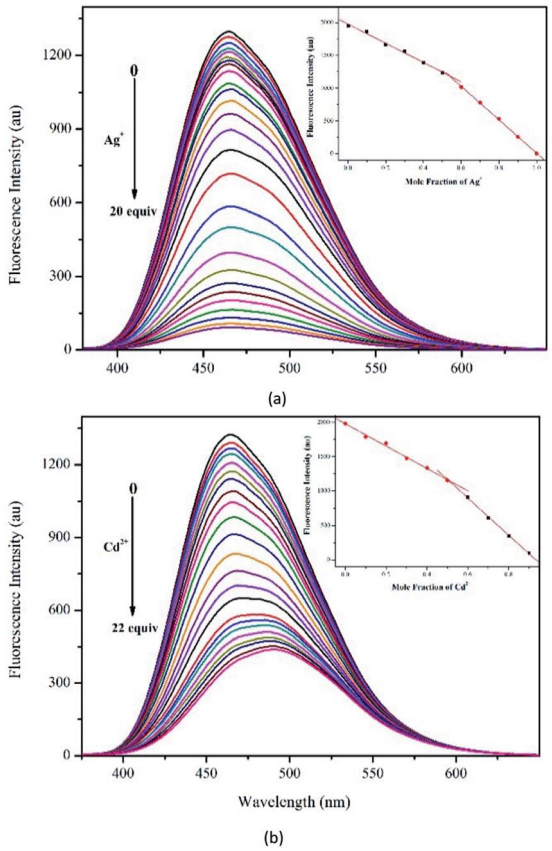

Fig. 4 The fluorescence intensity of probe **DQT** (10 μM) in CH_3OH/HEPES (9 : 1 v/v, pH = 7.30) buffer system upon incremental addition of Ag^+ (a) and Cd^{2+} (b). Job's curves were shown at the upper right corner.

Fluorescence recognition of DQT-Cd^{2+} complex to S^{2-}

In the interference test, the detection of Ag^+ was easily affected by other metal ions, and thus we focused on the response of Cd^{2+} and anions, including S^{2-}, HSO_3^-, SO_3^{2-}, SO_4^{2-}, Br^-, F^-, CO_3^{2-}, Cl^-, OAc^-, HCO_3^-, I^-, NO_2^- and NO_3^- in CH_3OH/HEPES (9 : 1 v/v, pH = 7.30) buffer system (λ_{ex} = 344 nm). In Fig. 5, only S^{2-} showed obvious fluorescence recovery with an enhancement efficiency of 64% and a blue shift from 490 to 465 nm. Competition experiments were performed to explore the effects of other anions on the recognition of S^{2-}. As exhibited in Fig. S8,† significant fluorescence recovery was observed upon the addition of 20 equiv. of S^{2-}. Obviously, these anions had no effect on the recognition of S^{2-}, especially sulfur-containing anions. Thus, **DQT**-Cd^{2+} showed high specificity for S^{2-}.

The fluorescence titration with S^{2-} was recorded in CH_3OH/HEPES (9 : 1 v/v, pH = 7.30) buffer system (λ_{ex} = 344 nm). In Fig. 6, the intensity of the strongest fluorescence emission peak gradually increased and blue-shifted as the S^{2-} concentration

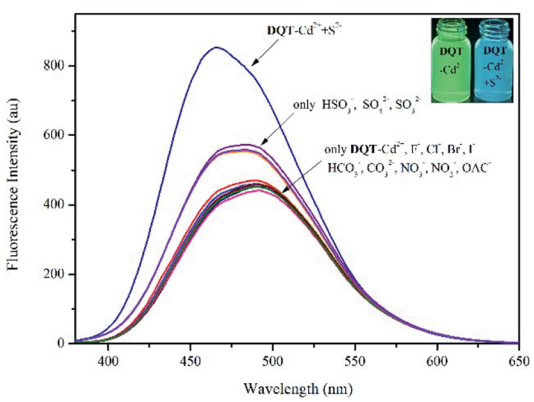

Fig. 5 Fluorescence spectra of **DQT**-Cd^{2+} (1×10^{-5} mol L^{-1}) with the addition of various anions (20 equiv.) in CH_3OH/HEPES (9 : 1 v/v, pH = 7.30) buffer system.

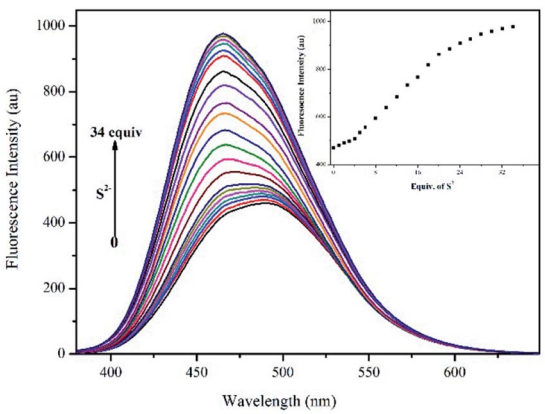

Fig. 6 Fluorescence spectra of **DQT**-Cd^{2+} (10 μM) with S^{2-} (0–34 equiv.) in CH_3OH/HEPES (9 : 1 v/v, pH = 7.30) buffer system (λ_{ex} = 344 nm). Inset: the plot of fluorescence intensity **DQT**-Cd^{2+} *versus* S^{2-}.

was increased to 34 equiv., after which it remained relatively constant. The LOD was calculated to be 11.50 μM by eqn (1) (Fig. S9,† $Y = 21.99 \times X + 420.56$, $R^2 = 0.9983$).

Reversibility of probe DQT for Cd^{2+} and S^{2-}

The reversibility was determined by alternating addition of Cd^{2+} and S^{2-}. As illustrated in Fig. 7, the fluorescence intensity was quenched to 33% and the fluorescence colour changed from blue to green observed by naked eye with the addition of Cd^{2+}. However, the addition of S^{2-} resulted in the recovery of the fluorescence intensity to about 64% and fluorescence colour change to blue. As the number of cycles increased, the recognition performance decreased gradually but still remained high after 3 cycles.

Effect of pH

As shown in Fig. 8, probe **DQT** exhibited excellent sequence selectivity and a red-shift at pH = 4–8 with the addition of Cd^{2+}, and the fluorescence was replied with the addition of S^{2-}. The selectivity of probe **DQT** was affected under highly acidic or alkaline conditions, probably due to changes in the structure of the probe and the loss of the coordination with ions.

DFT study

Gaussian 09 program was used for the density functional theory calculation at the level of B3LYP/6-31G (d, p) and B3LYP/LANL2DZ to gain a further insight into the photophysical properties and the nature of optical response of **DQT**, **DQT**-Ag^+ and **DQT**-Cd^{2+}. Fig. 9 showed the optimized structures and the electron dispersion of HOMO and LUMO. The molecular structure of probe **DQT** was planar, and most electrons in HOMO and LUMO were distributed on the 8-methoxyquinoline and quinolinylbenzothiazole groups, respectively. Its planarity was destroyed and the dihedral angles of quinolinobenzothiazole and 8-methoxyquinoline groups were 10° and 17° after coordinating with Ag^+ and Cd^{2+}, respectively. The electrons in HOMO were transferred to the binding site with Ag^+, which promoted the PET process and quenched the fluorescence. Similarly, the electrons in HOMO and LUMO were mainly concentrated on the quinolinylbenzothiazole group after coordination with Cd^{2+}, resulting in a red shift. The energy gaps of **DQT**, **DQT**-Ag^+ and **DQT**-Cd^{2+} were 3.78 eV, 3.57 eV and 3.38 eV, respectively, indicating that the binding with Cd^{2+} was more stable.

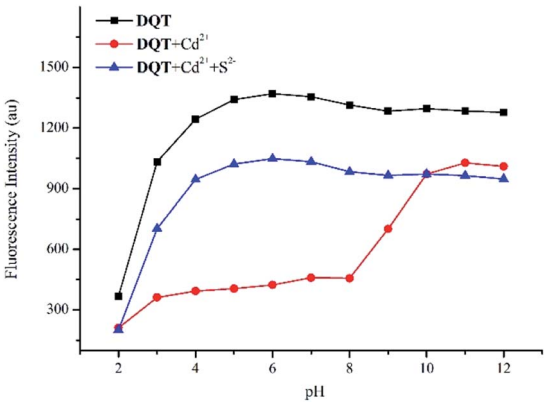

Fig. 8 Influences of the fluorescence intensity of probe **DQT** (10 μM) toward Cd^{2+} (20 equiv.) and S^{2-} (20 equiv.) at pH = 2–12 in CH_3OH/HEPES (9 : 1 v/v) buffer system at room temperature.

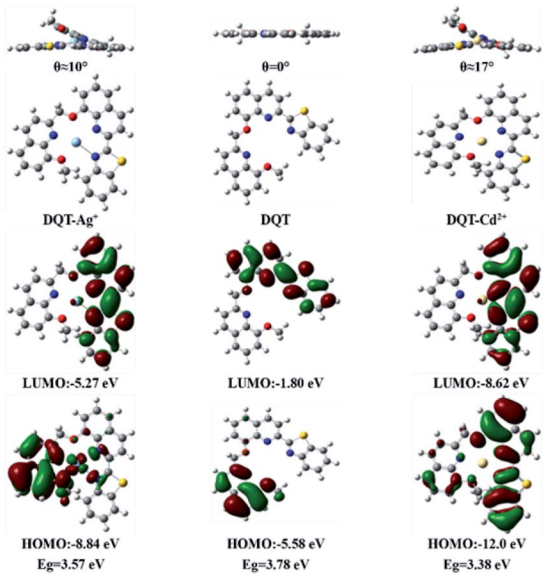

Fig. 9 Molecular orbital and electronic contributions of the relevant excitations.

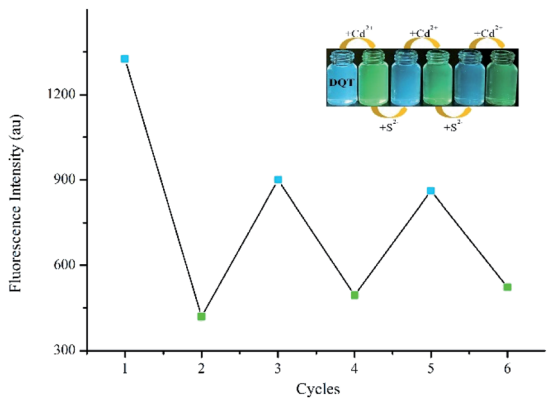

Fig. 7 Reversible changes in fluorescence intensity of probe **DQT** (10 μM) in CH_3OH/HEPES (9 : 1 v/v, pH = 7.30) buffer system upon alternate addition of Cd^{2+} and S^{2-}.

The possible mechanism

The possible mechanism is proposed as follows. The stoichiometry of the **DQT**-Ag^+ and **DQT**-Cd^{2+} complex is determined to be 1 : 1. Given the fluorescence quenching and no red shift of emission wavelength, the binding mode of probe **DQT** and Ag^+ conforms to the PET process. The coordination mechanism of probe **DQT** and Cd^{2+} can be attributed to ICT because the fluorescence emission wavelength is red-shifted after

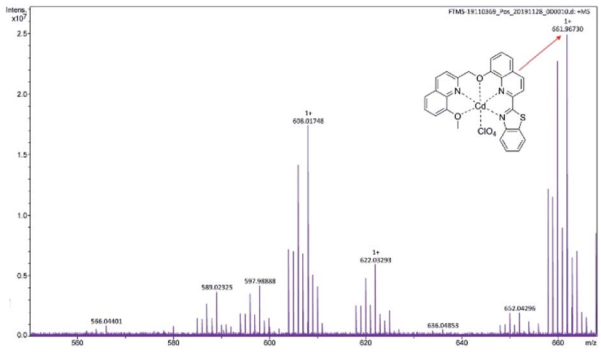

Fig. 10 ESI-MS spectra of **DQT**-Cd^{2+}.

coordination with Cd^{2+}.[34,42] Moreover, the molecular ion peak (ESI-MS) at 661.96730 [**DQT** + Cd^{2+} + ClO_4^-; *m*/*z* calcd for 661.97167] (Fig. 10) indicates an 1 : 1 complexation between probe **DQT** and Cd^{2+}, and thus it can be concluded that all nitrogen and oxygen atoms of the molecule participate in coordination. Due to the strong interaction between S^{2-} and Cd^{2+}, the overall fluorescence is recovered after the addition of S^{2-}, suggesting that S^{2-} can form CdS precipitate with Cd^{2+} and remove Cd^{2+} from **DQT**-Cd^{2+} complex. In summary, the Scheme 2 manifested the possible coordination mode.

Practical application on test strips

Filter paper strip test was carried out to determine the practicability of probe **DQT**. Filter paper strips were immersed in CH_3OH/HEPES (9 : 1 v/v, pH = 7.30) buffer system of **DQT** at a concentration of 1×10^{-3} M for 30 min and dried in air, and then smeared with Ag^+ and Cd^{2+} solution respectively. The fluorescence changes were observed under UV light. Fig. 11 showed that the fluorescence color of the test strip which treated with Cd^{2+} changed from blue (Fig. 11(b)) to green (Fig. 11(c)), while the fluorescence was quenched after treated with Ag^+ (Fig. 11(a)), suggesting that probe **DQT** could be used to distinguish for Ag^+ and Cd^{2+} by naked eye under UV light.

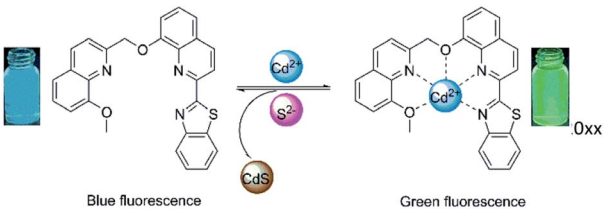

Scheme 2 The possible mechanism.

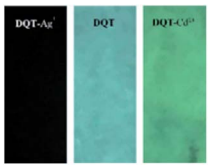

Fig. 11 Color changes on test paper (a) **DQT**-Ag^+; (b) **DQT**; (c) **DQT**-Cd^{2+} under UV light.

Conclusions

Herein, probe **DQT** was successfully synthesized for recognition of multiple ions. It showed fluorescence quenching towards Ag^+ based on the PET mechanism, but the complexation constant was low and the recognition of Ag^+ could be interfered by other ions. Probe **DQT** could also be used to detect Cd^{2+} based on the ICT mechanism with a red shift of 25 nm of the fluorescence emission wavelength in the same CH_3OH/HEPES (9 : 1 v/v, pH = 7.30) buffer system. The **DQT**-Cd^{2+} complex could be used for recognition of S^{2-}. Both Ag^+ and Cd^{2+} could form complexes with probe **DQT** with a coordination ratio of 1 : 1. Finally, filter paper strip test verified its practicability.

Conflicts of interest

There are no conflicts to declare.

Acknowledgements

We gratefully acknowledge the financial support from Applied Basic Research Programs of Shanxi Province (Grant No. 201801D221087), the Science Foundation of North University of China (No. 110121) and Program for Young Leaders of Disciplines in North University of China (Grant No. QX201806).

References

1 L. N. Xu, X. H. Yang, H. Y. Ding, S. H. Li, M. Li, D. Wang and J. L. Xia, *Mater. Sci. Eng., C*, 2019, **102**, 917.
2 Y. Y. Zhu, Q. Sun, J. W. Shi, H. Y. Xia, J. L. Wang, H. Y. Chen, H. F. He, L. Shen, F. Zhao and J. Zhong, *J. Photochem. Photobiol., A*, 2019, **389**, 112244.
3 J. H. Wang, Y. M. Liu, J. B. Chao, H. Wang, Y. Wang and S. M. Shuang, *Sens. Actuators, B*, 2020, **303**, 127216.
4 P. Liu, J. Liu, F. Yao, X. M. Zhan and X. P. Qi, *J. Photochem. Photobiol., B*, 2020, **202**, 111717.
5 Z. E. Chen, H. Zhang and Z. Iqbal, *Spectrochim. Acta, Part A*, 2019, **215**, 34.
6 D. K. Dang, S. Chandrasekaran, Y. T. Ngo, J. S. Chung, E. J. Kim and S. H. Hur, *Sens. Actuators, B*, 2018, **255**, 3284.
7 P. Ravichandiran, A. Boguszewska-Czubara, M. Masłyk, A. P. Bella, P. M. Johnson, S. A. Subramaniyan, K. S. Shim and D. J. Yoo, *Dyes Pigm.*, 2020, **172**, 107828.
8 M. X. Huang, C. H. Lv, Q. D. Huang, J. P. Lai and H. Sun, *RSC Adv.*, 2019, **9**, 36011.
9 Y. F. Tang, Y. Huang, Y. H. Chen, L. X. Lu, C. Wang, T. Sun, M. Wang, G. H. Zhu, Y. Yang, L. Zhang and J. L. Zhu, *Spectrochim. Acta, Part A*, 2019, **218**, 359.
10 A. Maity, U. Ghosh, D. Giri, D. Mukherjee, T. K. Maiti and S. K. Patra, *Dalton Trans.*, 2019, **48**, 2108.
11 L. I. Szekeres, S. Bálint, G. Galbács, I. Kálomista, T. Kiss, F. H. Larsen, L. Hemmingsen and A. Jancsó, *Dalton Trans.*, 2019, **48**, 8327.

12 P. Wang, Y. An and Y. W. Liao, *Spectrochim. Acta, Part A*, 2019, **216**, 61.
13 P. Wang, L. P. Duan and Y. W. Liao, *Microchem. J.*, 2019, **146**, 818.
14 Z. N. Lu, L. Wang, X. Zhang and Z. J. Zhu, *Spectrochim. Acta, Part A*, 2019, **213**, 57.
15 X. K. Li, Q. Y. Ming, R. Cai, T. L. Yue, Y. H. Yuan, Z. P. Gao and Z. L. Wang, *Food Control*, 2020, **109**, 106916.
16 N. Zhang and B. Hu, *Anal. Chim. Acta*, 2012, **723**, 54.
17 Y. Y. Liu, H. C. Li, B. Guo, L. J. Wei, B. Chen and Y. Y. Zhang, *Biosens. Bioelectron.*, 2017, **91**, 734.
18 W. D. Gao, Y. P. Zhang, H. Li and S. Z. Pu, *Tetrahedron*, 2018, **74**, 6299.
19 Y. Wang, X. F. Hou, Z. S. Li, C. H. Liu, S. S. Hu, C. M. Li, Z. H. Xu and Y. Wang, *Dyes Pigm.*, 2020, **173**, 107951.
20 Y. H. Yuan, L. X. Guo, Z. Z. Chen, Y. J. Zhu, L. H. Feng, W. Hua, M. Z. Tian, H. Y. Wang and F. Feng, *Microchem. J.*, 2019, **147**, 615.
21 C. L. Li, P. H. Lu, S. Y. Lin and A. T. Wu, *J. Photochem. Photobiol., A*, 2019, **385**, 112088.
22 J. Wang, Z. Y. Zhang, X. Gao, X. D. Lin, Y. Q. Liu and S. Wang, *Sens. Actuators, B*, 2019, **282**, 712.
23 S. J. Jiang, J. B. Qiu, S. B. Chen, H. Y. Guo and F. K. Yang, *Spectrochim. Acta, Part A*, 2020, **227**, 117568.
24 J. H. Wang, D. R. Gao, X. Y. Wang, Y. M. Lu, W. X. Shen and Y. Y. Lv, *Sens. Actuators, B*, 2019, **294**, 14.
25 D. J. Zhu, X. W. Yan, A. S. Ren, W. Cai, Z. H. Duan and Y. H. Luo, *Anal. Methods*, 2019, **11**, 2579.
26 T. Ma, F. J. Huo, Y. Wen, T. E. Glass and C. X. Yin, *Spectrochim. Acta, Part A*, 2019, **214**, 355.
27 C. Y. Zhao, J. Chen, D. L. Cao, J. L. Wang and W. B. Ma, *Tetrahedron*, 2019, **75**, 1997.
28 W. Q. Tang, Y. Z. Dai, B. Gu, M. Q. Liu, Z. J. Yi, Z. L. Li, Z. M. Zhang, H. Y. He and R. Y. Zeng, *Analyst*, 2020, **145**, 1427.
29 J. Han, X. Tang, Y. Wang, R. J. Liu, L. Wang and L. Ni, *Spectrochim. Acta, Part A*, 2018, **205**, 597.
30 P. Wang, J. Wu and C. H. Zhao, *Spectrochim. Acta, Part A*, 2020, **226**, 117600.
31 H. H. Song and Z. Zhang, *Dyes Pigm.*, 2019, **165**, 172.
32 J. F. Lv, G. Liu, C. B. Fan and S. Z. Pu, *Spectrochim. Acta, Part A*, 2020, **227**, 117581.
33 M. Banerjee, M. Ghosh, S. Ta, J. Das and D. Das, *J. Photochem. Photobiol., A*, 2019, **377**, 286.
34 Z. Liu, C. N. Peng, Z. X. Lu, X. F. Yang, M. S. Pei and G. Y. Zhang, *Dyes Pigm.*, 2015, **123**, 85.
35 Z. Liu, G. P. Li, Y. N. Wang, J. L. Li, Y. Mi, D. P. Zou, T. S. Li and Y. J. Wu, *Talanta*, 2019, **192**, 6.
36 L. F. Wang and Y. Qian, *J. Photochem. Photobiol., A*, 2019, **372**, 122.
37 T. M. Kawakami, Y. Mizuno, T. Inoue, S. Matsubara and T. Moriuchi, *Analyst*, 2019, **144**, 1140.
38 W. Y. Li, Z. C. Liu, B. Q. Fang, M. Jin and Y. Tian, *Biosens. Bioelectron.*, 2020, **148**, 111666.
39 S. Manna, P. Karmakar, S. S. Ali, U. N. Guria, S. K. Samanta, R. Sarkar, P. Dattab and A. K. Mahapatra, *Anal. Methods*, 2019, **11**, 1199.
40 M. Li, H. Chen, X. Liu, Y. L. Wang, N. N. Zhang and K. B. Zheng, *Tetrahedron Lett.*, 2019, **60**, 151219.
41 W. S. Na, P. Raj, N. Singh and D. O. Jang, *Tetrahedron Lett.*, 2019, **60**, 151075.
42 Q. L. Liu, L. X. Feng, C. X. Yuan, L. Zhang, S. M. Shuang, C. Dong, Q. Hu and M. M. Choi, *Chem. Commun.*, 2014, **50**, 2498.